Electronic Supplementary Material for "Imperfect vaccine and hysteresis"

Xingru Chen and Feng Fu

Contents

1 Vaccination dynamics in well-mixed populations

Concerning imperfect vaccination, whose effectiveness is denoted by ε, the ordinary differential equations for the SIR-V model are as follows.

$$\frac{dS}{dt} = -\beta SI, \tag{1}$$

$$\frac{dI}{dt} = \beta SI + (1-\varepsilon)\beta VI - \gamma I, \tag{2}$$

$$\frac{dV}{dt} = -(1-\varepsilon)\beta VI, \tag{3}$$

$$\frac{dR}{dt} = \gamma I. \tag{4}$$

Here S, I, R, and V stands for the fraction of susceptible, infected, recovered, and vaccinated individuals in the population. β is the disease transmission rate, and γ is the recovery rate. And $R_0 = \beta/\gamma$. The initial condition is

$$\begin{aligned} S(0) &= 1 - x, && (5)\\ V(0) &= x, && (6)\\ I(0) &= 0^+, && (7)\\ R(0) &= 0, && (8) \end{aligned}$$

where x stands for the population vaccination level. A routine calculation gives the implicit solutions with respect to $R(t)$:

$$\begin{aligned} S(t) &= (1-x)e^{-R_0 R(t)}, && (9)\\ V(t) &= xe^{(1-\varepsilon)R_0 R(t)}. && (10) \end{aligned}$$

Given that the identity $S(t) + V(t) + I(t) + R(t) = 1$ always holds, for $t \to \infty$ we obtain

$$(1-x)e^{-R_0 R(\infty)} + xe^{(1-\varepsilon)R_0 R(\infty)} + R(\infty) = 1. \quad (11)$$

A simple manipulation leads to the expression of x as a function of $R(\infty)$

$$x = \frac{R(\infty) + \exp[-R_0 R(\infty)] - 1}{\exp[-R_0 R(\infty)] - \exp[-(1-\varepsilon)R_0 R(\infty)]}. \quad (12)$$

Now we treat the vaccination dynamics as a two-stage game, that is, vaccination decisions (vaccination vs. nonvaccination) followed by disease outbreaks that determine the health outcomes of each individual. It follows that the infection risk for an unvaccinated individual, ω_0, and that for an vaccinated individual, ω_1, are just

$$\begin{aligned} \omega_0 &= 1 - \frac{S(\infty)}{S(0)} = 1 - \exp[-R_0 R(\infty)], && (13)\\ \omega_1 &= 1 - \frac{V(\infty)}{V(0)} = 1 - \exp[-(1-\varepsilon)R_0 R(\infty)], && (14) \end{aligned}$$

respectively. Let c be the relative cost of vaccination to infection. Up to a positive constant factor, the expected payoff for an unvaccinated individual and that for an vaccinated individual

are therefore

$$f_0 = -\omega_0, \tag{15}$$

$$f_1 = -c(1-\omega_1) - (1+c)\omega_1, \tag{16}$$

separately.

We first approach the vaccination game by considering the evolutionarily stable strategy (ESS). Consequently the two strategies, vaccination vs. nonvaccination, share the same payoff at ESS. As the equilibrium vaccination level x^* may be seen as the probability of getting vaccinated, we immediately derive a parametric relation between c and x^*.

$$c = \exp[-(1-\varepsilon)R_0R(\infty)] - \exp[-R_0R(\infty)], \tag{17}$$

$$x^* = \frac{R(\infty) + \exp[-R_0R(\infty)] - 1}{\exp[-R_0R(\infty)] - \exp[-(1-\varepsilon)R_0R(\infty)]}. \tag{18}$$

When $c = 0$ (vaccination incurs no cost), x^* coincides with the social optimum of vaccination coverage $\frac{R_0-1}{\varepsilon R_0}$. When $\varepsilon = 1$ (the vaccine is perfect), we can solve the ESS in explicit form $x^* = 1 + \frac{\ln(1-c)}{cR_0}$.

On the other hand, we can apply the replicator dynamics to analyze the problem. Owing to the fact that the final epidemic size $R(\infty)$ is implicitly dependent on the population vaccination level x, both f_0 and f_1 can be treated as functions of x. Denote the payoff difference by $F(x) = f_1(x) - f_0(x)$. The social imitation dynamics of vaccination behavior is therefore described by the replicator equation

$$\frac{dx}{dt} = x(1-x)F(x), \tag{19}$$

governing the time evolution of the fraction of vaccinated individuals, x, over epidemic seasons. Solving the fixed points of $F(x) = 0$ yields the possible interior equilibrium x^* and the same implicit equations which describe the dependence of x^* on c and ε through $R(\infty)$ as given above Eqs. (17) and (18). There can exist multiple interior equilibria of vaccination level x^* under certain parameter combinations of c and ε.

1.1 Proof: nonzero $R(\infty)$ is decreasing with the vaccination coverage $x > 0$

We proceed to prove that the nonzero final epidemic size $R(\infty) > 0$ is monotonically decreasing with the vaccination level $x > 0$. That is, $\frac{dR(\infty)}{dx} < 0$. For notational simplicity, let $r = R(\infty)$. We

rewrite (12) as

$$r = x[1 - e^{-(1-\varepsilon)R_0 r}] + (1-x)(1 - e^{-R_0 r}). \tag{20}$$

Further define

$$\begin{aligned} p_1(r) &= 1 - e^{-(1-\varepsilon)R_0 r}, & (21)\\ p_2(r) &= 1 - e^{-R_0 r}, & (22)\\ \phi(r) &= x p_1(r) + (1-x) p_2(r). & (23) \end{aligned}$$

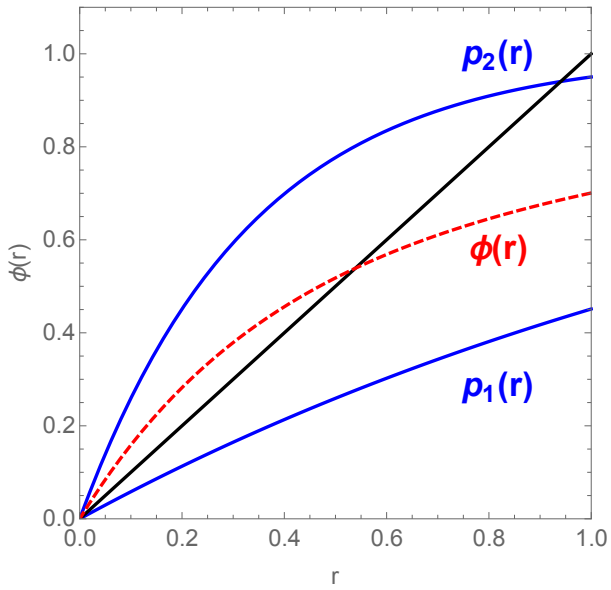

Figure S1: Illustrative plot of the fixed point problem.

It is easy to show that both p_1 and p_2 are increasing functions of r and that $p_1 < p_2$ when $r \in (0, 1)$. Then Eq. (20) becomes a fixed point problem (Fig. S1)

$$r = \phi(r). \tag{24}$$

Define $\varphi(r) = \phi(r) - r$. Take the derivative of $\varphi(r)$:

$$\varphi^{'}(r) = x(1-\varepsilon)R_0 e^{-(1-\varepsilon)R_0 r} + (1-x)R_0 e^{-R_0 r} - 1, \tag{25}$$

which is apparently a decreasing function of r. In particular,

$$\varphi'_{\max} = \varphi'(0) = (1-\varepsilon x)R_0 - 1 > 0, \tag{26}$$

$$\varphi'_{\min} = \varphi'(1) < x + (1-x) - 1 < 0. \tag{27}$$

The first inequality is guaranteed by the requirement of obtaining nonzero $R(\infty)$; otherwise, the fixed point problem would only has one unique zero solution. The second inequality is by the fact that $e^y > y$ for $y > 0$.

That is, $\varphi(r)$ first increasing then decreasing as r ranges from 0 to 1. Yet $\varphi(0) = 0$ and $\varphi(1) < x + (1-x) - 1 = 0$, forcing that $\varphi(r)$ has a unique root r^* in $(0,1)$. We remark that the fixed point r^* may be derived from the recursive equation

$$r_{n+1} = \phi(r_n), \tag{28}$$

where $r^* = \lim_{n\to\infty} r_n$. We are now turning to the proof that nonzero $R(\infty)$ is a monotonically decreasing function of x. Assume that there exists $0 < x < \tilde{x} < 1$, such that the corresponding $R(\infty) < \tilde{R}(\infty)$ and argue by contradiction. By substituting x and $\tilde{x}$ into (28), we obtain

$$r_1 = xp_1(r_0) + (1-x)p_2(r_0), \tag{29}$$

$$\tilde{r}_1 = \tilde{x}p_1(r_0) + (1-\tilde{x})p_2(r_0). \tag{30}$$

Given that $p_1(r) < p_2(r)$, we have

$$r_1 = x(p_1 - p_2) + p_2 > \tilde{x}(p_1 - p_2) + p_2 = \tilde{r}_1. \tag{31}$$

Repeating the iteration one more time gives rise to

$$r_2 = xp_1(r_1) + (1-x)p_2(r_1), \tag{32}$$

$$\tilde{r}_2 = \tilde{x}p_1(\tilde{r}_1) + (1-\tilde{x})p_2(\tilde{r}_1). \tag{33}$$

Recall that both $p_1(r)$ and $p_2(r)$ are increasing functions and thus $p_i(r_1) > p_i(\tilde{r}_1)$, for $i = 1, 2$. It follows that

$$r_2 > xp_1(\tilde{r}_1) + (1-x)p_2(\tilde{r}_1) > \tilde{r}_2. \tag{34}$$

By induction, we derive the inequality

$$\lim_{n\to\infty} r_n > \lim_{n\to\infty} \tilde{r}_n, \tag{35}$$

which implies that $R(\infty) > \tilde{R}(\infty)$, a contradiction.

1.2 Bistability condition

To gain further insight into understanding the bistability of equilibrium vaccination level x^*, we scrutinize Eqs. (17) and (18). These closed-form formulae allow us to perform a thorough bifurcation analysis based on the bistability condition.

If the vaccine is perfect, there corresponds only one equilibrium vaccination level x^* for $c \in (0, 1)$. In contrast, multiple equilibria can emerge if vaccine efficacy ε is below a threshold. To see this, we observe that $c(R(\infty))$ can become non-monotonic (Fig. S2a) as $R(\infty)$ increases from 0 to $R(\infty)_m$, where $R(\infty)_m \in (0, 1)$ is the unique root of

$$\exp(-R_0 R(\infty)) + R(\infty) - 1 = 0. \tag{36}$$

We employ here the result above that $R(\infty)$ is strictly decreasing with x whence its maximum value is realized at $x = 0$ (Fig. S2b). Define $y = \exp[-R_0 R(\infty)]$ and immediately we have $c(y) = y^{1-\varepsilon} - y$. Calculate the first two derivatives of $c(y)$:

$$\frac{dc}{dy} = (1-\varepsilon)y^{-\varepsilon} - 1, \tag{37}$$

$$\frac{d^2c}{dy^2} = -\varepsilon(1-\varepsilon)y^{-(1+\varepsilon)} < 0. \tag{38}$$

Observe that $y \in (\exp[-R_0 R(\infty)_m], 1)$. Therefore $c(R(\infty))$ is non-monotonic if and only if

$$(1-\varepsilon)\exp[\varepsilon R_0 R(\infty)_m] - 1 > 0, \tag{39}$$

which further yields

$$R(\infty)_m > -\frac{1}{\varepsilon R_0}\ln(1-\varepsilon). \tag{40}$$

Combined with Eq. (36), we get the lower bound of R_0 for this non-monotonicity to occur:

$$R_0 > -\frac{1}{\varepsilon}\frac{\ln(1-\varepsilon)}{1-(1-\varepsilon)^{\frac{1}{\varepsilon}}}. \tag{41}$$

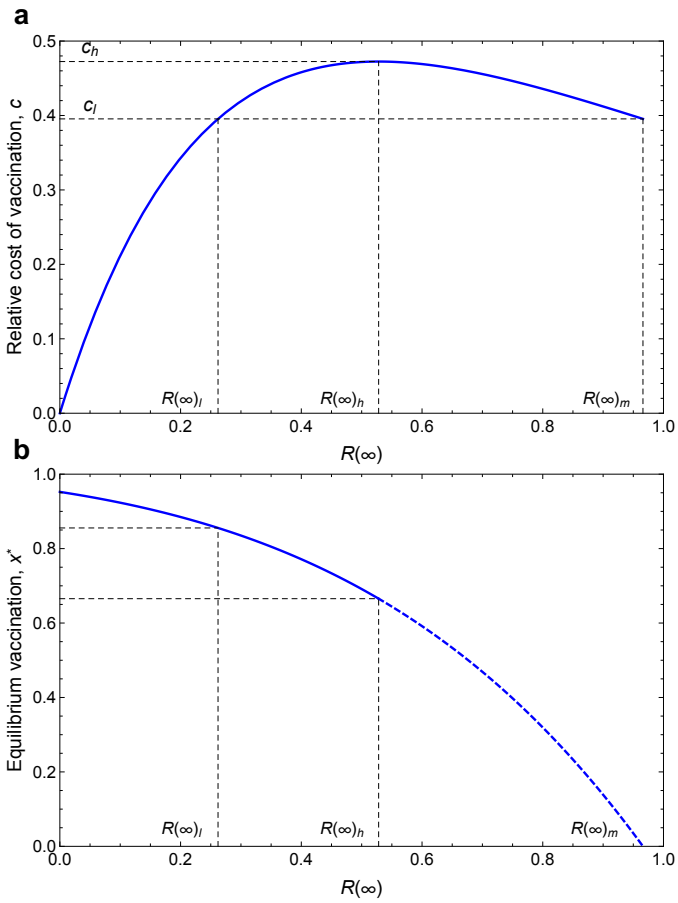

Figure S2: Graphic plots of (a) c and (b) x^* as a function of the final epidemic size $R(\infty)$. Parameters: $\varepsilon = 0.75$, $R_0 = 3.5$.

It is straightforward to show that $-\frac{1}{\varepsilon}\frac{\ln(1-\varepsilon)}{1-(1-\varepsilon)^{\frac{1}{\varepsilon}}}$ is an increasing function of ε. Hence in particular

$$R_0 > -\frac{1}{\varepsilon}\frac{\ln(1-\varepsilon)}{1-(1-\varepsilon)^{\frac{1}{\varepsilon}}} \mid_{\varepsilon\to 0} = \frac{e}{1-e}, \tag{42}$$

where $e \approx 2.71$ is the natural logarithm base.

On the other hand, when $c \to 0$, $R(\infty) \to 0$. Performing the L'Hospital rule to Eq. (18) gives rise to

$$x^* = \frac{R_0 - 1}{\varepsilon R_0}. \tag{43}$$

Given that $x^* \leq 1$ always holds, we obtain an upper bound of R_0:

$$R_0 \leq \frac{1}{1-\varepsilon}. \tag{44}$$

It remains to establish two threshold values for the relative cost of vaccination, c_l and c_h, such that there exists bistability of x^* on the interval (c_l, c_h). It is easy to see that c_l is the threshold of c for $x^* = 0$, satisfying:

$$c_l = \exp[-(1-\varepsilon)R_0 R(\infty)_m] - \exp[-R_0 R(\infty)_m], \tag{45}$$

where $R(\infty)_m$ is still the largest possible epidemic size with zero vaccination coverage. Meanwhile, c_h is the threshold of c above which zero vaccination coverage is the only stable population equilibrium (Fig. S2). By maximizing $c(y) = y^{1-\varepsilon} - y$, it turns out that

$$c_h = (1-\varepsilon)^{\frac{1-\varepsilon}{\varepsilon}} - (1-\varepsilon)^{\frac{1}{\varepsilon}} \tag{46}$$

1.3 Bifurcation analysis

Now we explain these results in more details. For $0 < c < c_l$ there exists a unique stable interior equilibrium. For $c_l < c < c_h$, there exist two interior equilibria, denoted by $0 < x_1 < x_2$ and we will demonstrate later that x_2 is stable while x_1 is unstable. The boundary fixed points $x = 0$ is stable and $x = 1$ is unstable. For $c > c_h$, no interior equilibria exist. Still $x = 0$ is stable and $x = 1$ is unstable.

The stability of interior equilibrium x_i is determined by the sign of $F'(x_i)$: if $F'(x_i) < 0$ it is

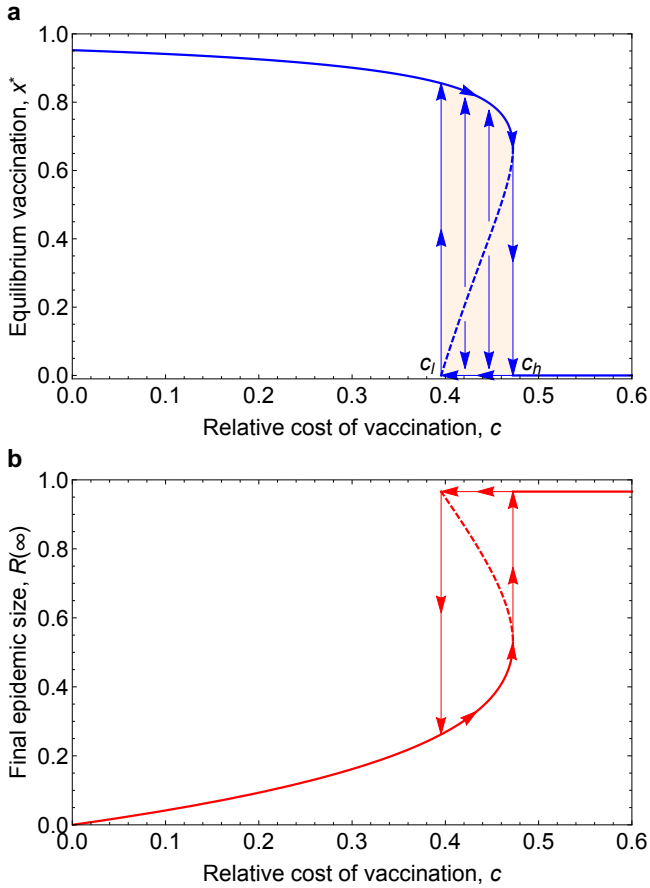

Figure S3: Bifurcation and hysteresis with respect to changes in the relative cost of vaccination, c. Parameters: $\varepsilon = 0.75$, $R_0 = 3.5$.

stable, otherwise unstable. Using the chain rule, we get

$$F'(x_i) = \frac{dF}{dR(\infty)} \frac{dR(\infty)}{dx}\bigg|_{x=x_i}. \tag{47}$$

For $0 < c < c_l$, we have $\frac{dF}{dR(\infty)} > 0$ and $\frac{dR(\infty)}{dx} < 0$. Thus the unique interior equilibrium is stable. For $c_l < c < c_h$, we have when $x_i = x_2$, $\frac{dF}{dR(\infty)} > 0$ and $\frac{dR(\infty)}{dx} < 0$ and hence x_2 is stable; when $x_i = x_1$, $\frac{dF}{dR(\infty)} < 0$ and $\frac{dR(\infty)}{dx} < 0$, and therefore x_1 is unstable (also see Fig. S2). For $c > c_h$, it is similar to check that the only stable population equilibrium is $x = 0$ (Fig. S3).

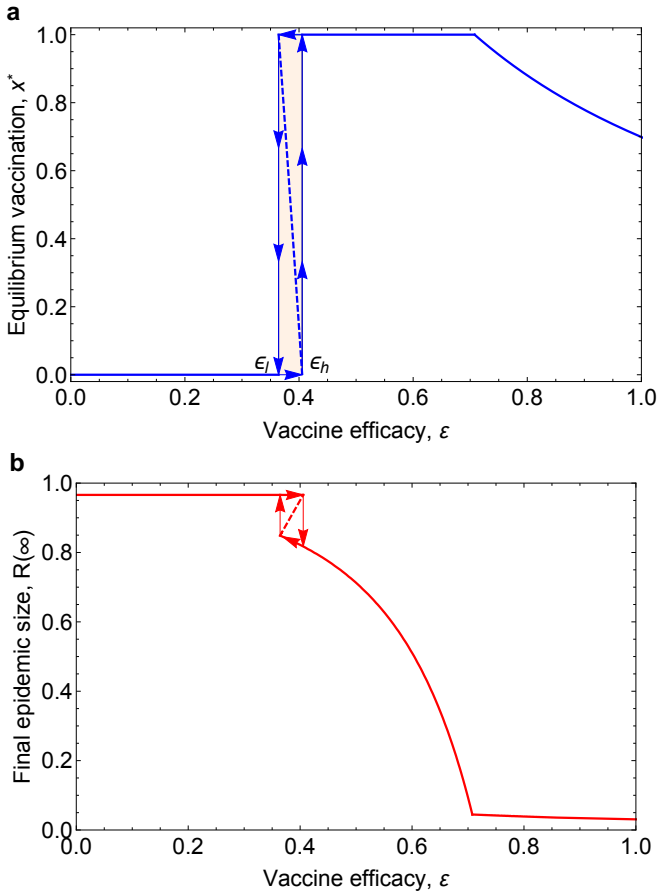

Figure S4: Bifurcation and hysteresis with respect to changes in the vaccine efficacy, ε. Panel (b) shows the final epidemic size $R(\infty)$ corresponding to the equilibrium vaccination level in Panel (a). Parameters: $c = 0.1$, $R_0 = 3.5$.

Bifurcation analysis of equilibrium vaccination levels with respect with changes in the vaccine efficacy, ε, for fixed cost of vaccination c, can be performed similarly as given above (Fig. S4). To do so, we just need to express the equilibrium x^* as a function of ε as follows.

$$\varepsilon = 1 + \frac{\ln\{c + \exp[-R_0 R(\infty)]\}}{R_0 R(\infty)}, \tag{48}$$

$$x^* = \frac{R(\infty) + \exp[-R_0 R(\infty)] - 1}{\exp[-R_0 R(\infty)] - \exp[-(1-\varepsilon) R_0 R(\infty)]}. \tag{49}$$

As shown in Fig. S4, the bifurcation diagrams and hysteresis phenomena are almost similar to these presented in the main text (Figs. 2 & 3), except that there exists an interesting yet counterintuitive overshooting behavior of vaccination coverage with respect to ε. Equilibrium vaccination coverage first increases – and even full coverage can be attained under certain model conditions (Fig. S4) – despite the decrease in vaccine efficacy from 100%. Depending on the combination of model parameters R_0 and c, these two threshold values ε_l and ε_h relevant to the resulting hysteresis loop can be determined accordingly (Fig. S4).

2 Model extensions

2.1 Vaccination dynamics on network populations

In addition to the spatial lattice populations considered in the main text, we simulate vaccination dynamics in network populations where individuals are connected by random graphs. As shown in Fig. S5, we confirm that similar hysteresis effect can also arise in random network populations.

2.2 Impact of co-evolving vaccine attitudes on vaccination dynamics in lattice populations

As the perceived risk or cost of vaccination is driven by individuals' attitudes toward vaccination, we incorporate into our basic model an opinion dynamics that coevolves with the vaccination uptake decisions. We consider two different opinions: one is vaccine-neutral attitude that concerns the real cost of vaccination, c; the opposite is vaccine-averse attitude that exaggerates the cost of vaccination by $\theta > 0$, with a perceived cost of vaccination $c + \theta$. Similar simulation method is used except that individuals will now imitate both the vaccine attitude and the uptake decision of a randomly chosen neighbor. Our results suggest that, as compared to the basic model, vaccination coverage is more sensitive to the increase in perceived cost of vaccination and also more difficult to recover in the presence of co-evolving vaccine altitudes (Fig. S6).

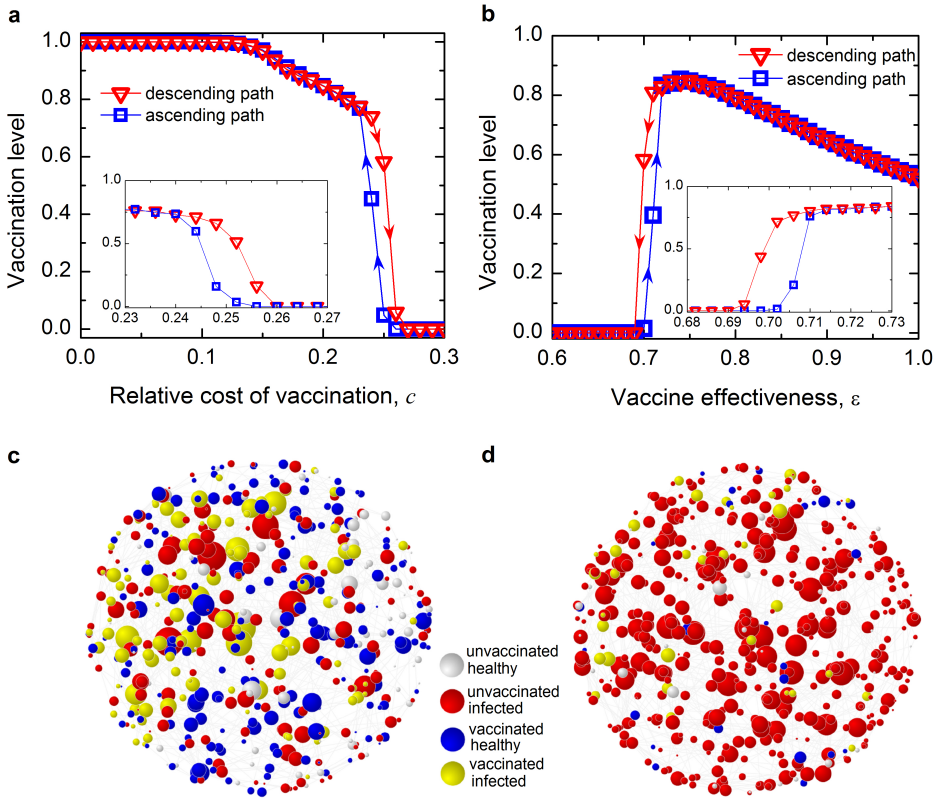

Figure S5: Hysteresis in random network populations. Shown are the occurrence of hysteresis loops with respect to changes in (a) the relative cost of vaccination, c, and (b) the effectiveness of vaccination, ε. The inset plots in (a) and (b) show the details of the corresponding hysteresis loops. Panels (c) and (d) are network snapshots of population states, respectively, in the descending and ascending path of the hysteresis loop in panel (a) for $c = 0.25$ and $\varepsilon = 0.75$. Parameters: average network degree $d = 4$, number of infection seeds $I_0 = 10$, transmission rate $\beta = 0.51$, recovery rate $\gamma = 1/3$, (a), (b) $N = 1000$, (c), (d) $N = 500$, (a) $\varepsilon = 0.75$, (b) $c = 0.2$. Simulation results are averaged over 100 independent runs.

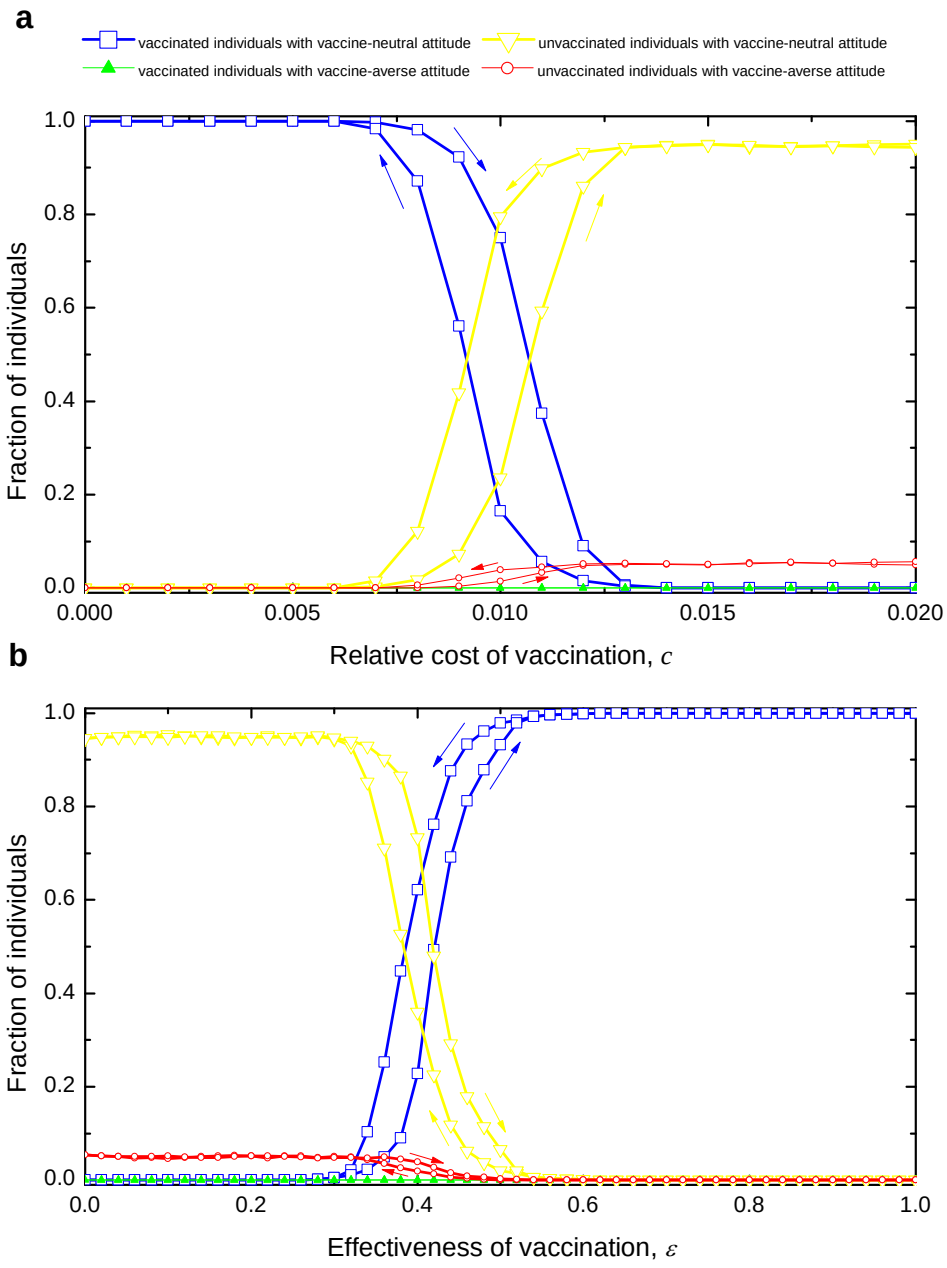

Figure S6: Coevolution of vaccine attitude and uptake behavior in lattice populations. Shown are the hysteresis loops with respect to changes in (a) the relative cost of vaccination, c, and in (b) the effectiveness of vaccination, ε. The directions of the hysteresis loops are indicated by the arrows. Parameters: lattice size 50×50 with the von Neumann neighborhood, equal initial frequency of each type of individuals, number of infection seeds $I_0 = 30$, transmission rate $\beta = 0.0375$, recovery rate $\gamma = 0.1$, $\theta = 0.1$, (a) $\varepsilon = 0.4$, (b) $c = 0.01$. Results are averaged over 400 independent runs.

2.3 Vaccination dynamics in age-structured populations and waning of vaccine protection

Of particular interest is to study secondary vaccine failure in the context of childhood diseases (such as mumps and measles). Here, vaccine failure is depicted as waning of initial vaccine protection over time elapsed since vaccination. As most types of children immunizations are scheduled more or less within 12 months of birth, we assume that vaccination is given shortly after birth. For simplicity, we further suppose that a fraction x of each age cohort are vaccinated, essentially at birth.

To understand the impact of vaccine failures due to declining efficacy of protection, we incorporate into the basic model an age structure that depicts different mixing contacts and thus heterogeneous risks of infections for members of each age group. Without loss of generality, we consider n age classes, and their mixing contacts are described by the matrix $\Phi = \{\phi_{ij}\}_{n\times n}$. The force of infection for individuals in age class a is $\beta_a \sum_{j=1}^{n} \phi_{aj} I_j$. Therefore, the age-structured epidemiological model is given by:

$$\frac{dS_a}{dt} = -\beta_a S_a \left(\sum_{j=1}^{n} \phi_{aj} I_j \right), \tag{50}$$

$$\frac{dI_a}{dt} = [\beta_a S_a + \beta_a (1-\varepsilon_a) V_a] \left(\sum_{j=1}^{n} \phi_{aj} I_j \right) - \gamma_a I_a, \tag{51}$$

$$\frac{dV_a}{dt} = -\beta_a (1-\varepsilon_a) V_a \left(\sum_{j=1}^{n} \phi_{aj} I_j \right), \tag{52}$$

$$\frac{dR_a}{dt} = \gamma_a I_a, \tag{53}$$

for age class $a = 1, 2, \cdots, n$, respectively. For notational convenience, we use vectors of age-specific model parameters to denote transmission rates $\hat{\beta} = [\beta_1, \beta_2, \cdots, \beta_n]$, recovery rates $\hat{\gamma} = [\gamma_1, \gamma_2, \cdots, \gamma_n]$, and vaccine efficacies $\hat{\varepsilon} = [\varepsilon_1, \varepsilon_2, \cdots, \varepsilon_n]$, respectively. The population proportion of each age class is denoted by $\hat{\alpha} = [\alpha_1, \alpha_2, \cdots, \alpha_n]$. We have $\sum_{i=1}^{n} \alpha_i = 1$. The parameter ε_a quantifies the degree of waning of vaccine protection for individuals in age class a who have received vaccination at birth.

More general cases where a fraction x of each age cohort are vaccinated at age b can be analyzed analogously; we just need to set the initial conditions $V_a(0) = 0$ for age cohort $a < b$ and $V_a(0) = x\alpha_a$ for $a \geq b$.

Specifically, we consider five age classes in our analysis, corresponding to the age intervals $[0\,4]$, $[5\,9]$, $[10\,14]$, $[15\,19]$, and $[20\,75]$. Under equilibrium age distribution, the size of these age groups is given by $[5N_0, 5N_0, 5N_0, 5N_0, 55N_0]$, where N_0 is the number of newborns. This leads to $\hat{\alpha} = [1, 1, 1, 1, 11]/15$.

For each age class a, the risks of infection for vaccinated vs. unvaccinated can be calculated as follows.

From Eq. (53), we get $\sum_{j=1}^{n} \phi_{aj} I_j(t) = \sum_{j=1}^{n} \frac{dR_j(t)}{dt} \phi_{aj}/\gamma_j = \frac{d(\sum_{j=1}^{n} R_j(t)\phi_{aj}/\gamma_j)}{dt}$. Dividing it with Eq. (50) separately on both sides, we obtain

$$\frac{dS_a}{S_a} = -\beta_a d(\sum_{j=1}^{n} R_j(t)\phi_{aj}/\gamma_j). \tag{54}$$

Integrating both sides from 0 to ∞, we arrive at

$$\frac{S_a(\infty)}{S_a(0)} = \exp\left[-\beta_a \left(\sum_{j=1}^{n} R_j(\infty)\phi_{aj}/\gamma_j)\right)\right]. \tag{55}$$

Similarly, we get

$$\frac{V_a(\infty)}{V_a(0)} = \exp\left[-\beta_a(1-\varepsilon_a) \left(\sum_{j=1}^{n} R_j(\infty)\phi_{aj}/\gamma_j)\right)\right]. \tag{56}$$

Using the condition $S_a(0)+V_a(0) = S_a(\infty)+V_a(\infty)+R_a(\infty) = \alpha_a$, we obtain the following set of transcendental equations for the final epidemic size $R_a(\infty)$ in age class a, for $a = 1, 2, \cdots, n$, which can be solved numerically:

$$\begin{aligned} R_a(\infty) &= \alpha_a - \alpha_a(1-x)\exp\left[-\beta_a \left(\sum_{j=1}^{n} R_j(\infty)\phi_{aj}/\gamma_j)\right)\right] \\ &\quad -\alpha_a x \exp\left[-\beta_a(1-\varepsilon_a) \left(\sum_{j=1}^{n} R_j(\infty)\phi_{aj}/\gamma_j)\right)\right]. \end{aligned} \tag{57}$$

The risk of infection, ω_0^a, for an unvaccinated individual in age class a can be calculated as

$$\omega_0^a = 1 - \frac{S_a(\infty)}{S_a(0)} = 1 - \exp\left[-\beta_a \left(\sum_{j=1}^{n} R_j(\infty)\phi_{aj}/\gamma_j)\right)\right]. \tag{58}$$

The risk of infection, ω_1^a, for a vaccinated individual in age class a can be calculated as

$$\omega_1^a = 1 - \frac{V_a(\infty)}{V_a(0)} = 1 - \exp\left[-\beta_a(1-\varepsilon_a)\left(\sum_{j=1}^{n} R_j(\infty)\phi_{aj}/\gamma_j\right)\right]. \tag{59}$$

Then the expected payoff of an unvaccinated individual throughout one's lifetime is

$$f_1(x) = -c + \sum_{a=1}^{n} \alpha_a[(-1)\cdot\omega_1^a]. \tag{60}$$

Similarly, the expected payoff of an unvaccinated individual is

$$f_0(x) = \sum_{a=1}^{n} \alpha_a[(-1)\cdot\omega_0^a]. \tag{61}$$

As before, the social imitation dynamics of vaccination is described by the replicator equation:

$$\frac{dx}{dt} = x(1-x)[f_1(x) - f_0(x)].$$

We perform bifurcation analysis across the space of model parameters, in particular, with respect to changes in the relative cost of vaccination and the waning efficacy of vaccination. As shown in the main text, we find that hysteresis effect can also arise in age-structured populations with secondary vaccine failure.